# Tail risk in government bond markets and ECB asset purchases*

*Xin Zhang,*[(a)] *Bernd Schwaab*[(b)]

[(a)] Sveriges Riksbank, Research Division

[(b)] European Central Bank, Financial Research

January 28, 2016

**Abstract**

This paper derives a novel observation-driven model that allows for time variation in the tail shape parameter of the Generalized Pareto Distribution. The tail shape dynamics are driven by the score of the predictive log-likelihood. Monte Carlo experiments suggest that the model reliably captures tail index variation in a variety of different settings. In an empirical study of sovereign bond yields at a high frequency, we demonstrate that the European Central Bank's Securities Markets Programme was able to temporarily lower the tail risk associated with holding certain sovereign bonds during the euro area sovereign debt crisis between 2010–2012.

**Keywords:** tail risk, observation-driven models, extreme value theory, European Central Bank (ECB), Securities Markets Programme (SMP).

**JEL classification:** *C22, G11.*

*Author information: Xin Zhang, Research Division, Sveriges Riksbank, SE 103 37 Stockholm, Sweden, Email: xin.zhang@riksbank.se. Bernd Schwaab, Financial Research, European Central Bank, Sonnemannstrasse 22, 60314 Frankfurt, Germany, Email: bernd.schwaab@ecb.int. We thank Simone Manganelli, Daniele Massacci, and David Veredas for comments. The views expressed in this paper are those of the author and they do not necessarily reflect the views or policies of the Sveriges Riksbank or European Central Bank.

# 1 Introduction

We propose a novel observation-driven model that introduces time series dynamics into the tail shape parameter of the Generalized Pareto Distribution (GPD). The GPD is of considerable interest to financial economists, as it is the only non-degenerate density that approximates the distribution of data exceedances beyond a given threshold; see, for example, Davidson and Smith (1990), Embrechts, Klüppelberg, and Mikosch (1997), and McNeil, Frey, and Embrechts (2010, Chapter 7). As a result, it plays a similarly central role in the study of extremes as the normal distribution does in the study of non-tail observations; see Rocco (2014) for a recent survey of extreme value theory (EVT) methods.

In our model, the tail shape dynamics are driven by the score of the predictive log-likelihood. So-called Generalized Autoregressive Score (GAS) models were developed in their full generality in Creal, Koopman, and Lucas (2013); see also Harvey (2013) for a textbook treatment. In this setting, the time-varying parameter is perfectly predictable one step ahead. This feature makes the model observation-driven in the terminology of Cox (1981). The likelihood is known in closed-form through a standard prediction error decomposition, and parameter estimation is straightforward.

Extensive Monte Carlo experiments suggest that our score-driven model reliably captures tail shape variation in a variety of settings. In addition, the treatment of non-tail observations is an important concern in the dynamic modeling of the tail shape parameter. We therefore consider different approaches to the treatment of such observations in each simulation: deletion, modeling as missing without information on the tail, and as a draw from a censored density. We find that the simple deletion of missing values is appropriate if the tails are sufficiently fat. Modeling non-tail observations as missing works well if mean reversion in the tail shape process is strong, regardless of the fatness in the tail. Modeling the tail shape dynamics by a censored distribution performs best when the tail is less fat, and tail observations become less frequent.

We apply our score-driven modeling framework to sovereign bond yields at a high frequency for five euro area countries: Greece, Ireland, Italy, Portugal, and Spain. Based on

these estimates we demonstrate that the European Central Bank (ECB)'s Securities Markets Programme (SMP) was able to temporarily lower the tail risk associated with holding most of these bonds during the euro area sovereign debt crisis between 2010–2012. This is relevant since elevated tail risks alone can force institutional investors and market makers to retreat from a given market, particularly if value-at-risk constraints are binding; see, for example, Vayanos and Vila (2009) and Adrian and Shin (2010). The effects studied here are on top of the impact on the conditional mean and variance of bond yields as documented in Ghysels, Idier, Manganelli, and Vergote (2016) and Eser and Schwaab (2016).

Several studies investigate the dynamic behavior of the tail index. Quintos, Fan, and Phillips (2001) derive formal tests for time-variation in the tail index. A number of subsequent studies apply these tests to financial time series data. For example, Werner and Upper (2004) identify several breaks in the tail behavior of high-frequency German Bund future returns. Similarly, Galbraith and Zernov (2004) demonstrate that certain regulatory changes in U.S. equity markets altered the tail index dynamics of equities returns, while Wagner (2005) argues that changes in government bond yields exhibit time-variation in the tail shape for both the U.S. and the euro area. Another promising strand of EVT literature exploits the high-dimensional panel structure of many datasets. For example, Kelly (2014) develops a power law model for cross-sectional tail risk that takes a GARCH-type autoregressive form. Building on this framework, Kelly and Jiang (2014) link the common fluctuations in equity tail risk to other asset returns and macro-economic aggregates. Finally, (dynamic) EVT has been applied in the study of systemic risk; see Hartmann, Straetmans, and de Vries (2004, 2007), and Allen, Bali, and Tang (2012).

The methodological part of this paper is closest to Massacci (2014). Massacci proposes an observation-driven time series model for both the tail and scale parameters in the GPD distribution of a univariate time series. Both parameters evolve in a bivariate system, and are updated jointly based on the scaled score of the tail shape parameter. This approach is a welcome addition to the econometrician's toolkit. However, it assumes that researchers are unwilling to work with pre-filtered data. This is not the case; see McNeil and Frey (2000), Poon, Rockinger, and Tawn (2004), Brownlees and Engle (2015), Lucas, Schwaab, and Zhang

(2014, 2016), and others. If the data are de-volatized based on a sensible volatility model in a first step, the scale of the GPD becomes fixed (at unity), leaving only one time-varying parameter to model. No bivariate updating of parameters is necessary, and the number of time-invariant parameters to be estimated decreases from six to three.

We proceed as follows. Section 2 introduces the statistical model. Section 3 provides evidence from an extensive Monte Carlo study. Section 4 applies the model to euro area sovereign bond yields. Section 5 concludes.

# 2 Statistical model

## 2.1 Time-varying tail risk

This section introduces time variation into the tail shape parameter $\xi_t > 0$ of the Generalized Pareto Distribution (GPD). The probability density function (pdf) of a GPD distributed random variable $x_t > 0$ is given by

$$p(x_t; \delta, \xi_t) = \frac{1}{\delta}\left(1 + \xi_t \frac{x_t}{\delta}\right)^{-\frac{1}{\xi_t}-1}, \tag{1}$$

where $x_t = y_t - \tau > 0$ is the so-called peak-over-threshold (POT), or exceedance, of data $y_t$ over a pre-determined threshold $\tau$, $\delta > 0$ is an additional scale (variance) parameter, and $\xi_t$ is the tail shape parameter; see, for example, McNeil, Frey, and Embrechts (2010). If $y_t - \tau \leq 0$, we may consider $x_t$ as missing, or censored, see Section 2.2 below. As a result, exceedances $x = (x_1, \ldots, x_T)$ and data $y = (y_1, \ldots, y_T)$, $t = 1, \ldots, T$, are univariate time series at the same frequency. The cumulative distribution function (cdf) and the log-likelihood of $x_t$ is given by

$$P(x_t; \delta, \xi_t) = 1 - \left(1 + \xi_t \frac{x_t}{\delta}\right)^{-\frac{1}{\xi_t}}, \qquad l(x_t; \delta, \xi_t) = -\ln(\delta) - \left(1 + \frac{1}{\xi_t}\right)\ln\left(1 + \xi_t \frac{x_t}{\delta}\right), \tag{2}$$

respectively.

We assume that the pdf of $y_t$, $g(y_t)$, is a fat-tailed distribution with time-varying tail

index $\alpha_t$, such as, for example, a univariate Student's t distribution with $\nu_t = \alpha_t = 1/\xi_t$ degrees of freedom. In this case the cumulative distribution function $G(y_t)$ can be expressed as $G(y_t) = G(\tau) + (1 - G(\tau))P(x_t)$ for sufficiently high values of $\tau$. As a result, all interesting tail behavior is captured by $p(x_t; \delta, \xi_t)$.[1]

Following Creal, Koopman, and Lucas (2013) and Harvey (2013), we endow $\xi_t$ with score-driven (GAS) dynamics using the derivative of the log conditional observation density (1). We ensure positive values of $\xi_t$ by specifying $\xi_t = \exp(f_t)$. The transition dynamics for $f_t$ are given by

$$f_{t+1} = \omega + \sum_{i=0}^{p-1} a_i s_{t-i} + \sum_{j=0}^{q-1} b_j f_{t-j}, \tag{3}$$
$$s_t = \mathcal{S}_t \nabla_t, \quad \nabla_t = \partial \ln p(x_t | \mathcal{F}_{t-1}; f_t, \psi) / \partial f_t,$$

where $\omega = \omega(\psi)$ is a fixed intercept, and $a_i = a_i(\psi)$ and $b_j = b_j(\psi)$ are fixed scalar parameters that depend on the vector $\psi$ containing all time invariant parameters in the model.

For the remainder of the paper, we make three empirical choices. First, we select the inverse conditional Fisher information of the GPD distribution as our scaling function, $\mathcal{S}_t = \mathrm{E}[\nabla_t^2 | \mathcal{F}_{t-1}; f_t, \psi]^{-1} = \mathrm{E}[-\partial \nabla_t (x_t | \mathcal{F}_{t-1}; f_t, \psi) / \partial f_t]^{-1}$. Creal, Koopman, and Lucas (2013) and Creal, Schwaab, Koopman, and Lucas (2014) demonstrate that this choice of scaling function results in a stable model, and effectively yields a Gauss-Newton update of $f_t$ over time. Second, we consider a fixed $\delta = 1$ throughout the paper. This corresponds to the common practise of using volatility-filtered data before considering tail risk dynamics. If volatility clustering is not accounted for, movements in the tail may be confounded with movements in the conditional variance; see, for example, McNeil and Frey (2000). Finally, we assume $p = q = 1$ in (3), such that $a = a_0$ and $b = b_0$. Higher order terms are rarely necessary in practise; see Creal et al. (2013). To ensure stationarity of the factor process, we restrict $0 < b < 1$.

[1] The choice of threshold is subject to a well-known bias-efficiency tradeoff; see, for instance, McNeil, Frey, and Embrechts (2010). In theory, the limit distribution of exceedances holds exactly only as the threshold $\tau \to +\infty$. A higher threshold, however, also implies a smaller number of exceedances, and consequently an increased sampling error in the estimation of the tail shape parameter. We address this issue by considering multiple choices for $\tau$ in our empirical application. The 10% and 5% empirical quantile are common choices.

## 2.2 Treatment of non-tail observations

This section discusses three different approaches to the handling of non-tail observations $y_t \leq \tau$, and provides the resulting expressions for the conditional score $\nabla_t$ and scaling function $\mathcal{S}_t$ in (3). We consider the performance of these three approaches in our simulation experiments in Section 3.

First, we simply decide to delete the missing entries in the univariate time series. This yields a substantially shorter time series for $x$. In this case, closed-form expressions for the score $s_t$ and the scaling function $\mathcal{S}_t$ can be derived as

$$\nabla_t = \frac{1}{\xi_t} \ln\left(1 + \xi_t \frac{x_t}{\delta}\right) - (\xi_t + 1)\frac{x_t}{\delta + \xi_t x_t}, \tag{4}$$

$$\mathcal{S}_t = \frac{(1 + 2\xi_t)(1 + \xi_t)}{2\xi_t^2}, \tag{5}$$

where, again, $\mathcal{S}_t = \mathrm{E}[-\partial \nabla_t(x_t|\mathcal{F}_{t-1}; f_t, \psi)/\partial f_t]^{-1}$ is the inverse conditional Fisher information quantity for $x_t$. We refer to Appendix A1 for the derivation of (4) – (5). Deleting non-tail observations before applying (1) – (5) is straightforward, and in line with the spirit of EVT in the absence of time variation in the tail index; see McNeil, Frey, and Embrechts (2010, Chapter 7). One immediately downside of this approach, however, is that $\xi_t$ is unavailable for all $y_t \leq \tau$.

Second, we calculate the scaled score (4) – (5) only if $x_t$ is observed, and assign a zero value if $x_t$ is missing. This is similar to the approach considered in Creal, Schwaab, Koopman, and Lucas (2014). The updating equation becomes

$$f_{t+1} = \omega + a \cdot \mathrm{I}(x_t > 0)\mathcal{S}_t \nabla_t + b \cdot f_t. \tag{6}$$

As a result, $f_t = \ln(\xi_t)$ slowly reverts back to its unconditional mean $\omega/(1-b)$ in the absence of new information from the tail. The updating equation (6) takes into account that $\xi_t$ evolves as a continuous process which governs the tail behavior of each $y_t$. An estimate of $\xi_t$ is now available for all data $y_t$.

Finally, we use a censored distribution to model the exceedance and to derive the score;

see, for example, Davidson and Smith (1990) and Massacci (2014). In this case, observations $y_t \leq \tau$ generate the POT values $x_t = 0$. This approach allows us to incorporate information in the tail as well as from the center of the distribution. We consider the truncated distribution

$$p(x_t; \delta, \xi_t) = \mathrm{I}(x_t > 0) \left[ (1+\tau)^{-\frac{1}{\xi_t}} \frac{1}{\delta} \left( 1 + \xi_t \frac{x_t}{\delta} \right)^{-\frac{1}{\xi_t}-1} \right] + \mathrm{I}(x_t = 0) \left( 1 - (1+\tau)^{-\frac{1}{\xi_t}} \right). \quad (7)$$

The respective log-likelihood is

$$\begin{aligned} \ell(x_t; \delta, \xi_t) &= \mathrm{I}(x_t > 0) \left[ -\frac{1}{\xi_t} \ln(1+\tau) - \ln(\delta) - \left( 1 + \frac{1}{\xi_t} \right) \ln \left( 1 + \xi_t \frac{x_t}{\delta} \right) \right] \\ &+ \mathrm{I}(x_t = 0) \ln(1 - (1+\tau)^{-\frac{1}{\xi_t}}). \end{aligned} \quad (8)$$

The score-driven update of $f_t = \ln \xi_t$ becomes slightly more involved in this case. The score and scaling function are now given by

$$\begin{aligned} \nabla_t &= \mathrm{I}(x_t > 0) \left[ \frac{1}{\xi_t} \ln(1+\tau) + \frac{1}{\xi_t} \ln \left( 1 + \xi_t \frac{x_t}{\delta} \right) - (\xi_t + 1) \frac{x_t}{\delta + \xi_t x_t} \right] \\ &- \mathrm{I}(x_t = 0) \left[ \frac{(1+\tau)^{-\frac{1}{\xi_t}}}{1 - (1+\tau)^{-\frac{1}{\xi_t}}} \frac{1}{\xi_t} \ln(1+\tau) \right], \end{aligned} \quad (9)$$

and

$$\mathcal{S}_t = \left[ \frac{2\xi_t^2 (1+\tau)^{-\frac{1}{\xi_t}}}{(1+2\xi_t)(1+\xi_t)} + \frac{(1+\tau)^{-\frac{1}{\xi_t}}}{1 - (1+\tau)^{-\frac{1}{\xi_t}}} \frac{1}{\xi_t^2} \ln(1+\tau)^2 \right]^{-1}, \quad (10)$$

respectively. Since (9) and (10) are available in closed form, the transition equation for $f_t$ is straightforward.[2] Modeling the tail index as the inverse tail shape $\alpha_t = 1/\xi_t$ in a score-driven way leads to equivalent expressions for the score and the same scaling function.

### 2.2.1 Explanatory covariates

This section extends the score-driven dynamics for the time-varying tail shape to include lagged values of economic variables as additional conditioning variables. For example, ECB asset purchases may help explain the time variation in the right tail shape. As an extension,

[2] Computer code will eventually be available on `http://www.gasmodel.com`.

we consider score-driven dynamics (9) – (10) with factor dynamics that include ECB asset purchases,

$$f_{t+1} = \omega + a \cdot s_t + b \cdot f_t + c \cdot \Delta\text{SMP}_t + d \cdot \Delta\text{SMP}_{t-1} + e \cdot \Delta\text{SMP}_{t-2}, \tag{11}$$

where the additional right-hand side variables $\Delta\text{SMP}_t$ are daily changes in purchase volumes in €billion of par value. Purchase amounts (in levels) or respective dummy variables are alternative conditioning variables. Intraday values are held constant at the daily levels. We consider the extended specification (11) in Section 4.

# 3 Simulation study

This section presents our Monte Carlo results. We are particularly interested in the question which treatment of non-tail observations is appropriate.

We chose the Student's $t$ distribution $y_t \sim \text{t}(\nu)$ as our fat tailed distribution $g(y_t)$, and consider three values for the degrees of freedom parameter, $\nu = 3, 5, 7$. The threshold $\tau$ is the 90% percentile of the random sample generated from a $t(3)$ and $t(5)$ distribution, and the 95% percentile when the sample is generated from the $t(7)$ distribution (for which the tail is less fat). The exceedance sample contains $x_t \sim \text{GPD}(0, \delta, \xi_t)$ if $y_t > \tau$, and zero (missing) otherwise. The GPD distributed random variables are drawn as $x_t = \delta \frac{u_t^{-\xi_t} - 1}{\xi_t}$, where $u_t \sim \text{U}[0, 1]$ is uniform.

Each simulation uses a different path for the tail shape parameter $\xi_t = \exp(f_t)$. We consider seven data generating processes (DGP). The first four processes are standard stylized dynamics in the literature. The final three processes consider random draws of $f_t$ subject to different parameters $\psi$.

(1) Constant: $\xi_t = 0.9$,

(2) Sine: $\xi_t = 0.5 + 0.4 \cos(2\pi t/200)$,

(3) Fast Sine: $\xi_t = 0.5 + 0.4 \cos(2\pi t/20)$,

(4) Step: $\xi_t = 0.9 - 0.5(t > 500)$,

(5) sGPD$^d$ : (ignore missings) $f_{t+1} = \omega + a\mathcal{S}_t\nabla_t + bf_t$,

(6) sGPD$^m$ : (zero score) $f_{t+1} = \omega + a \cdot \mathrm{I}(x_t > 0)\mathcal{S}_t\nabla_t + bf_t$,

(7) sGPD$^c$ : (censored likelihood): $f_{t+1} = \omega + a\mathcal{S}_t\nabla_t + bf_t$,

where the parameters in simulation settings (5) – (7) are chosen in two different ways, as

$$\begin{aligned} \psi_1 &: \omega = -0.025, a = 0.01, b = 0.97, \delta = 1; \\ \psi_2 &: \omega = 0.01, a = 0.12, b = 0.85, \delta = 1. \end{aligned}$$

As a result, the tail risk dynamics under parameter vector $\psi_1$ are more persistent than in the model with $\psi_2$; note the higher value for $b$. In addition to exhibiting faster mean reversion, the tails are also fatter under $\psi_2$, as the unconditional mean of $f_t$, $\omega/(1-b)$, is substantially higher.

We end up with $4+2\times3 = 10$ stochastic GPDs, in three environments ($\nu = 3, 5, 7$). This yields 30 data generating processes. For each DGP, we draw 100 simulation samples of $y$ with $10,000$ observations each. As a result, approximately 1,000 ($t(\nu = 3, 5)$) or 500 ($t(\nu = 7)$) tail observations are used to construct POT values. Our main metric for evaluating model performance is Mean Absolute Error, MAE $= \frac{1}{ST}\sum_{s=1}^{S}\sum_{t=1}^{T}|\hat{\xi}_{st} - \xi_{st}|$, where $\hat{\xi}_{st}$ is the estimated dynamic tail parameter in simulation $s$, $\xi_{st}$ is the true tail shape, $S$ is the number of simulations, and $T$ is the number of observations in each draw.

Table 1 presents the main MAE simulation outcomes. We focus on three main findings. First, simply deleting missing values (our first approach) seems to be permissible as long as the tails are sufficiently fat. When $\nu = 3$, the respective factor estimates are close to the underlying true processes in many cases. Even if the true tail dynamics come from a censored-likelihood model, the sGPD$^d$ and sGPD$^m$ approaches still deliver close estimates. Modeling non-tail observations as missing, without information about the tail, works well if mean reversion in the tail shape process is strong ($\psi_2$).

As the degrees of freedom parameter increases and the sample size decreases ($\nu = 7$), the appropriateness of simply deleting missing values in $x$ becomes less clear. In all DGPs under $\psi_1$, the sGPD$^c$ model now outperforms the other approaches; see columns 6, 8, and 10. This

Table 1: **Simulation results: Mean Absolute Error**

The table reports mean absolute error (MAE) statistics for 12 DGPs (columns) and three estimation approaches (rows), in three environments (top, middle, and bottom panels). The hit variable $\mathrm{I}(y_t > \tau)$ is simulated from a $t(3)$, $t(5)$, and $t(7)$. We consider 100 simulations for each DGP, and a time series $y$ of $10,000$ observations in each simulation. Different approaches to the treatment of non-tail observations are indicated in the respective rows. sGPD$^d$ deletes missing vales, sGPD$^m$ assigns a zero value to the score at missing values, and sGPD$^c$ uses a censored density. Model performance is measured by the MAE from the true $\xi_t$ in each draw. The number in bold indicates minimum MAE among the four approaches considered. For DGPs (5)–(8), two sets of parameters $\psi_1$ and $\psi_2$ apply.

| Model | (1) | (2) | (3) | (4) | (5)-$\psi_1$ | (5)-$\psi_2$ | (6)-$\psi_1$ | (6)-$\psi_2$ | (7)-$\psi_1$ | (7)-$\psi_2$ |
|---|---|---|---|---|---|---|---|---|---|---|
| | | | | | $t$ distributed, $\nu = 3$ | | | | | |
| sGPD$^d$ | 0.049 | **0.202** | 0.259 | **0.151** | **0.045** | **0.097** | **0.038** | **0.100** | 0.044 | 0.136 |
| | (0.037) | (0.016) | (0.006) | (0.044) | (0.022) | (0.064) | (0.021) | (0.031) | (0.018) | (0.017) |
| sGPD$^m$ | **0.046** | 0.293 | 0.260 | 0.274 | 0.054 | 0.534 | 0.040 | 0.123 | **0.043** | **0.136** |
| | (0.037) | (0.042) | (0.008) | (0.040) | (0.028) | (0.139) | (0.029) | (0.052) | (0.024) | (0.020) |
| sGPD$^c$ | 0.359 | 0.255 | **0.255** | 0.249 | 0.092 | 0.619 | 0.090 | 0.528 | 0.061 | 0.300 |
| | (0.008) | (0.001) | (0.001) | (0.002) | (0.013) | (0.065) | (0.008) | (0.010) | (0.006) | (0.006) |
| | | | | | $t$ distributed, $\nu = 5$ | | | | | |
| sGPD$^d$ | 0.048 | **0.201** | 0.258 | **0.152** | 0.043 | **0.082** | 0.036 | **0.101** | 0.039 | 0.108 |
| | (0.034) | (0.015) | (0.006) | (0.046) | (0.022) | (0.037) | (0.021) | (0.032) | (0.019) | (0.015) |
| sGPD$^m$ | **0.045** | 0.297 | 0.259 | 0.280 | 0.057 | 0.566 | 0.036 | 0.117 | 0.036 | **0.106** |
| | (0.035) | (0.040) | (0.012) | (0.046) | (0.026) | (0.154) | (0.022) | (0.047) | (0.018) | (0.016) |
| sGPD$^c$ | 0.433 | 0.256 | **0.257** | 0.249 | **0.041** | 0.695 | **0.021** | 0.603 | **0.019** | 0.313 |
| | (0.007) | (0.001) | (0.001) | (0.002) | (0.005) | (0.064) | (0.005) | (0.008) | (0.003) | (0.005) |
| | | | | | $t$ distributed, $\nu = 7$ | | | | | |
| sGPD$^d$ | 0.069 | **0.209** | 0.260 | 0.066 | 0.058 | **0.142** | 0.050 | 0.097 | 0.052 | 0.096 |
| | (0.046) | (0.026) | (0.009) | (0.049) | (0.031) | (0.076) | (0.034) | (0.046) | (0.032) | (0.033) |
| sGPD$^m$ | **0.062** | 0.314 | **0.259** | **0.059** | 0.060 | 0.504 | 0.043 | **0.088** | 0.045 | **0.090** |
| | (0.044) | (0.113) | (0.007) | (0.046) | (0.030) | (0.221) | (0.032) | (0.047) | (0.029) | (0.029) |
| sGPD$^c$ | 0.477 | 0.260 | 0.261 | 0.477 | **0.039** | 0.740 | **0.022** | 0.646 | **0.020** | 0.344 |
| | (0.006) | (0.001) | (0.001) | (0.006) | (0.010) | (0.090) | (0.005) | (0.010) | (0.002) | (0.005) |

is not surprising. When the tail observations are less frequent and contain less information about the (thinner) tail, then the censored-likelihood model benefits from being able to take into account information from non-tail observations as well. If the tails are fatter ($\psi_2$), the first two approaches are again appropriate.

Second, the standard deviations about the MAE statistics are typically larger in the first two rows than for the censored-likelihood approach. This difference in standard errors points towards a loss of efficiency that occurs when we discard observations (as in the first approach), or model them by a zero value for the score (the second approach). Again, the censored-likelihood approach uses non-tail observations to at least some degree, implying less variation across simulations for these estimates.

Table 2: **Simulation results: Mean Squared Error**

The table reports mean squared error (MSE) statistics for 12 DGPs (columns) and three estimation approaches (rows), in three environments (top, middle, and bottom panels). The hit variable $\mathrm{I}(y_t > \tau)$ is simulated from a $t(3)$, $t(5)$, and $t(7)$. We consider 100 simulations for each DGP, and a time series $y$ of $10,000$ observations in each simulation. Different approaches to the treatment of non-tail observations are indicated in the respective rows. sGPD$^d$ deletes missing vales, sGPD$^m$ assigns a zero value to the score at missing values, and sGPD$^c$ uses a censored density. The number in bold indicates minimum MAE among the four approaches considered. For DGPs (5)–(8), two sets of parameters $\psi_1$ and $\psi_2$ apply.

| Model | (1) | (2) | (3) | (4) | (5)-$\psi_1$ | (5)-$\psi_2$ | (6)-$\psi_1$ | (6)-$\psi_2$ | (7)-$\psi_1$ | (7)-$\psi_2$ |
|---|---|---|---|---|---|---|---|---|---|---|
| | | | | | $t$ distributed, $\nu = 3$ | | | | | |
| sGPD$^d$ | 0.004 | **0.057** | 0.086 | **0.034** | **0.004** | **0.052** | **0.003** | **0.039** | 0.004 | 0.033 |
| | (0.006) | (0.010) | (0.007) | (0.015) | (0.004) | (0.085) | (0.004) | (0.027) | (0.003) | (0.008) |
| sGPD$^m$ | **0.004** | 0.127 | 0.086 | 0.124 | 0.005 | 0.933 | 0.004 | 0.119 | **0.004** | **0.033** |
| | (0.005) | (0.053) | (0.009) | (0.319) | (0.007) | (1.039) | (0.010) | (0.340) | (0.007) | (0.010) |
| sGPD$^c$ | 0.129 | 0.081 | **0.081** | 0.076 | 0.010 | 0.882 | 0.008 | 0.315 | 0.004 | 0.117 |
| | (0.006) | (0.001) | (0.001) | (0.002) | (0.002) | (0.613) | (0.002) | (0.027) | (0.001) | (0.006) |
| | | | | | $t$ distributed, $\nu = 5$ | | | | | |
| sGPD$^d$ | 0.004 | **0.058** | 0.085 | **0.040** | 0.003 | **0.030** | 0.002 | **0.044** | 0.003 | 0.019 |
| | (0.005) | (0.011) | (0.009) | (0.052) | (0.003) | (0.035) | (0.003) | (0.058) | (0.003) | (0.005) |
| sGPD$^m$ | **0.004** | 0.131 | 0.088 | 0.104 | 0.006 | 0.961 | 0.002 | 0.060 | 0.002 | **0.018** |
| | (0.005) | (0.051) | (0.040) | (0.062) | (0.006) | (0.720) | (0.003) | (0.074) | (0.002) | (0.004) |
| sGPD$^c$ | 0.187 | 0.082 | **0.082** | 0.099 | **0.003** | 0.960 | **0.001** | 0.408 | **0.001** | 0.113 |
| | (0.006) | (0.001) | (0.001) | (0.003) | (0.001) | (0.399) | (0.000) | (0.061) | (0.000) | (0.004) |
| | | | | | $t$ distributed, $\nu = 7$ | | | | | |
| sGPD$^d$ | 0.012 | **0.062** | 0.088 | 0.008 | 0.009 | **0.111** | 0.004 | 0.033 | 0.005 | 0.017 |
| | (0.035) | (0.016) | (0.012) | (0.010) | (0.027) | (0.179) | (0.005) | (0.056) | (0.005) | (0.010) |
| sGPD$^m$ | **0.006** | 0.155 | **0.086** | **0.006** | 0.006 | 0.821 | 0.003 | **0.033** | 0.003 | **0.015** |
| | (0.008) | (0.171) | (0.008) | (0.008) | (0.009) | (0.895) | (0.004) | (0.063) | (0.004) | (0.007) |
| sGPD$^c$ | 0.228 | 0.087 | 0.087 | 0.228 | **0.003** | 1.059 | **0.001** | 0.443 | **0.001** | 0.128 |
| | (0.005) | (0.001) | (0.001) | (0.005) | (0.002) | (0.571) | (0.000) | (0.070) | (0.000) | (0.004) |

Finally, the results are overall not too sensitive to which exact model is employed for inference on $\xi_t$. For example, the censored-likelihood approach is accurate even if the true model is formulated differently. In other words, even (slightly) misspecified score-driven models appear to work well. Again, this is not surprising. Blasques, Koopman, and Lucas (2015) prove that score-based parameter updates always reduce the local Kullback-Leibler divergence between the true conditional density and the (potentially misspecified) model-implied conditional density, and are in this sense optimal from an information theoretic perspective. Tables 1 and 2 suggest that slightly misspecified models can still work well in practise.

Table 2 presents the mean squared error outcomes, $\mathrm{MSE} = \frac{1}{ST}\sum_{s=1}^{S}\sum_{t=1}^{T}(\hat{\xi}_{st} - \xi_{st})^2$,

where $S$ and $T$ are as defined above. The MSE statistics correspond to a quadratic loss function, and punish large errors more heavily than MAE. The MSEs are qualitatively similar to the MAE outcomes in terms of relative accuracy. Again, the censored likelihood approaches perform well, particularly when the tails are fat, but not extremely fat. In all three cases, the estimated static parameters tend to be close to the true parameters if the estimated model coincides with the DGP used for the simulation.

# 4 Time-varying tail risk and asset purchases

We apply our dynamic GPD model to study the impact of asset purchases within the ECB's SMP on the tail risk of holding certain sovereign bonds. In practise, the tail risk of rapidly deteriorating government bond prices are not only borne by investors, but also by the dealers who make these markets. If uncertainty and tail risks become substantial, for example owing to debt sustainability or contagion concerns, then tail risks alone could force institutional investors and market makers to retreat, particularly if value-at-risk constraints are binding; see, for example, Vayanos and Vila (2009) and Adrian and Shin (2010).

## 4.1 ECB non-standard monetary policies

The absence of "depth and liquidity" in a subset of sovereign bond markets severely hinders a balanced, even transmission of a central bank's monetary policy stance across different countries in a monetary union. The SMP had the objective of helping to restore the monetary policy transmission mechanism by addressing the malfunctioning of certain government bond markets during the euro area sovereign debt crisis between 2010–2012; see, for instance, González-Páramo (2011). Implicit in the concept of malfunctioning markets is the notion that government bond yields can be unjustifiably high and volatile; see Eser et al. (2012) and Eser and Schwaab (2016). SMP purchases were made during a particularly severe sovereign debt crisis, when sovereign yields in several euro area countries were at a high, on the rise, and volatile. During this phase, the targeted securities met little private sector demand. The purchases were undertaken during the most intense phases of the debt crisis and in the

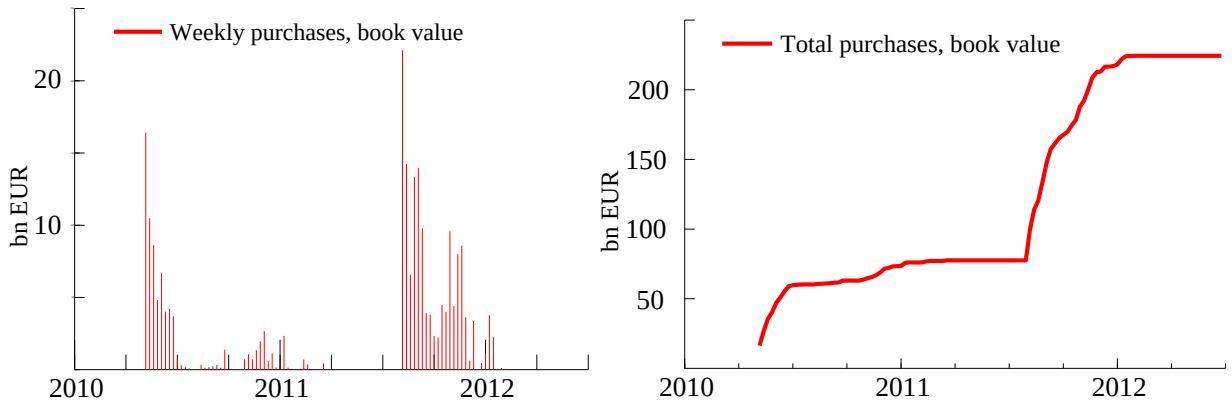


Figure 1: Weekly and total SMP purchase amounts.

The figure plots the book value of settled SMP purchases as of the end of a given week. We report weekly purchases across countries (left panel) as well as the cumulative amounts (right panel). Maturing amounts are excluded.

markets most affected by the crisis.

Figure 1 plots weekly total purchases across countries as well as their accumulated book value over time. Noticeably, the weekly purchase data are unevenly spread over time. The SMP was announced on 10 May 2010 and focused on Greek, Irish, and Portuguese debt securities. The program was extended to include Italian and Spanish bonds on 8 August 2011. Between 10 May 2010 and Spring 2012 there are long periods during which the SMP was open but inactive. Approximately €214 billion (bn) of bonds were acquired within the SMP between 2010 and early 2012. The SMP's daily cross-country breakdown of the purchase data is confidential at the time of writing. We use the confidential daily and country-specific data for this study.

The introduction of the SMP was subject to significant controversy, both outside and within the Eurosystem, i.e., the ECB and all National Central Banks (NCBs). The extent of the controversy within the Eurosystem became evident with the resignation of the Bundesbank President in February 2011 and an ECB Executive Board member in September 2011. The SMP was replaced by the Outright Monetary Transactions (OMTs) program on 6 September 2012. The SMP and the OMTs are related but different programs, see Cœuré (2013). No purchases were made within the OMT program. Instead, the mere announcement of that program was sufficient to calm financial markets and helped end the most acute phase

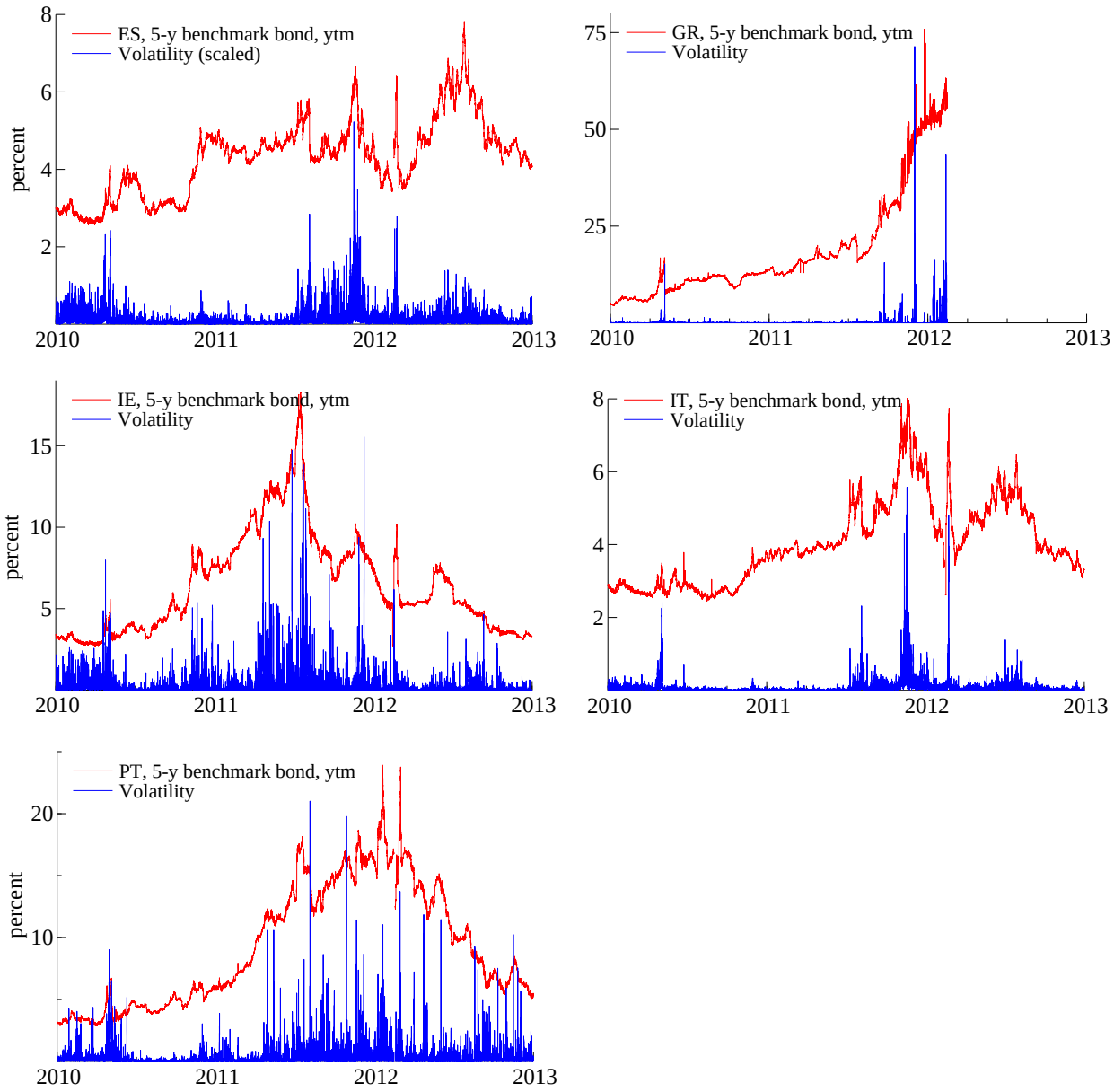


Figure 2: Five-year benchmark bond yields and volatility

Five-year benchmark bond yields and respective volatility estimates for Spain (ES), Greece (GR), Ireland (IE), Italy (IT), and Portugal (PT). Yields are in percentage points and are sampled at the 15 minute interval. Volatility estimates are based on a t-GAS volatility model; see Table 3 for the respective parameter estimates. Greek bonds discontinued trading after 02 March 2012, and experienced a credit event on 09 March 2012.

of the sovereign debt crisis; see, for instance, ECB (2013) and Lucas et al. (2014, 2016).

## 4.2 Volatility and tail shape estimates

Figure 2 plots the yield-to-maturity of five-year benchmark bonds for five euro area countries between 04 January 2010 and 31 December 2012, sampled at the 15 minute interval.[3] During the debt crisis, some yields exhibited occasional large and sudden moves (of up to 200 bps at a daily frequency), leading to strong volatility spikes. Announcement effects of the SMP program are visible in the yield data: five-year yields dropped by -773 bps in Greece, -139 bps in Ireland, and -226 bps in Portugal on 10 May 2010; and by -97 bps in Spain and -93 bps in Italy on 8 August 2011, measured as the difference between Monday 6pm and the preceding Friday at 6pm. In addition, the credit event for Greek bonds on 09 March 2012 appears to have led to pronounced temporary spikes in yield levels and volatility in the other four markets.

We use a standard t-GAS(1,1) volatility model to pre-filter our data before EVT estimation. The univariate volatility model is specified as

$$\begin{aligned} \bar{x}_t &\sim \mathrm{t}(\bar{x}_t; \sigma_t^2, \nu), \quad \ln(\sigma_t^2) = f_t^v, \\ f_{t+1}^v &= \omega_v + a_v \cdot s_{v,t} + b_v \cdot f_t^v, \end{aligned} \tag{12}$$

where $\bar{x}_t$ is the recursively demeaned (but not yet devolatized) change in the quoted yield of a certain bond, $\nu$ is the degrees of freedom (robustness) parameter, and $s_{v,t}$ is the scaled score from a t-distribution; see Creal et al. (2013) for details. A key feature of the Student's t-GAS(1,1) model, which differentiates it from a conditionally Gaussian (GARCH) model, is a weighting term that lessens the impact of occasional extreme observations. Such extreme observations commonly occur during a sovereign debt crisis, particularly at a high frequency. EVT estimation is based on $x_t = \bar{x}_t/\hat{\sigma}_t$, where $\hat{\sigma}_t$ is the filtered volatility estimate from (12).

Figure 2 reports our volatility estimates at the 15 minute frequency, in addition to bond yields. Volatility is high throughout 2010-2011 in Greece, Ireland, and Portugal, and peaks somewhat later around 2011Q4 in Italy and Spain. Greek bond volatility is most pronounced

[3]Bond data are obtained from Thomson Reuters. We consider the midpoint between executable quotes if ask and bid prices, quoted in yields.

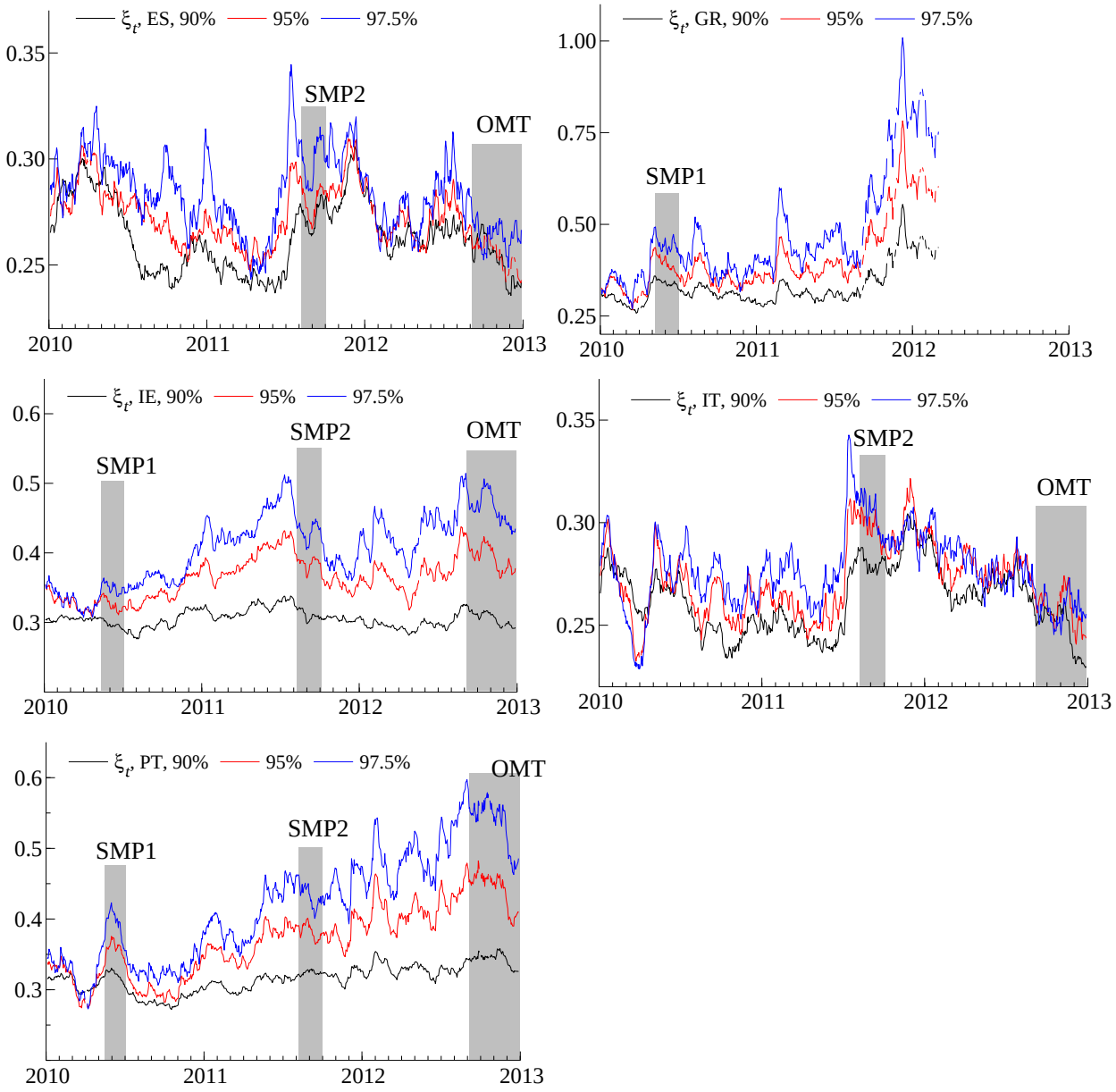


Figure 3: Tail risk dynamics in five euro area countries

Estimates of the time-varying tail shape parameter $\xi_t$ at different levels of $\tau$, corresponding to the 10%, 5%, and 2.5% quantile, for Spain (ES), Greece (GR), Ireland (IE), Italy (IT), and Portugal (PT). Daily estimates are obtained as the median value of the estimates at the 15 minute frequency. Shaded areas in 2010 and 2011 refer to frequent asset purchases within the SMP; see Figure 1. The shared area in late 2012 marks the period after the announcement of the technical details of the ECB's OMT programme on 06 September 2012. Greek bonds discontinued trading after 02 March 2012, and experienced a credit event on 09 March 2012.

in early 2012.

Figure 3 plots the respective estimates of $\xi_t$ corresponding to changes in the yield of a given country's five-year benchmark bond. We consider different thresholds, based on the

10%, 5%, and 2.5% empirical quantile of $x_t$. Bond yields are sampled at the 15 minute frequency between 8AM and 6PM; see Ghysels et al. (2016) for a similar approach. Grey shaded areas in 2010 and 2011 in Figure 3 mark periods of focussed SMP purchases in the respective markets, cf. Figure 1. The shaded area in late 2012 marks the time after the announcement of the technical details of the ECB's OMT. The tail index estimates suggest that periods of focussed asset purchases might be associated with reductions in the fatness of the right tail (i.e., $\xi_t$ decreased), at least in some cases. The effects are the most visible for Greek bonds. These bonds exhibited the highest yields and were subject to a particularly elevated level of stress between 2010–2012. Specifically, the second quarter of 2010 appears to be an exception to the otherwise upwards trend in tail risk. Greek bonds ultimately experienced a credit event on 09 March 2012.

The top panel of Table 3 reports the parameter estimates for our volatility models (12). The estimates indicate that yield changes at the 15 minute interval are fat tailed, in all five markets. In all cases, the estimates of $\nu$ converge from above to 2.5, which we have chosen as a lower bound for that parameter to prevent numerical instability that may occur as $\nu \downarrow 2$. In addition, the volatility processes are persistent, with $b_v > 0.9$ in all cases.

The middle panel of Table 3 presents the parameter estimates for our baseline score-driven tail shape model (3). We report the model parameters associated with the censored likelihood approach (7) – (10), as this approach performed well in our simulations as reported in Section 2.2, and allows us to obtain an estimate of $\xi_t$ at each point in time. The tail shape parameter estimates indicate fat tails, with median values of $\exp(\omega/(1-b))$ as reported in the last column of the bottom panel of Table 3. Overall, tail fatness is in line with what is suggested by the t-GAS volatility models, and suggests that t-distributions with $\nu \approx 2-3$ are appropriate for modeling changes in euro area bond yields at 15-minute intervals between 2010–2012. The tail shape processes are persistent, with typical values of $b > 0.95$.

The bottom panel of Table 3 presents the estimation results for the GAS-X specification (11) which allows for additional explanatory covariates. None of the additional coefficients for SMP variables are statistically significant according to their t-values. In addition, most log-likelihoods are only marginally higher than for specification (3), with the exception of

Table 3: Parameter estimates

The top panel presents parameter estimates for five univariate t-GAS volatility models (12). The middle panel refers to the tail shape parameter model (9) – (10). The bottom panel presents parameter estimates for the extended tail shape model (11) which includes additional variables as explanatory covariates. Rows labeled ES, GR, IE, IT, and PT refer to Spanish, Greek, Irish, Italian, and Portuguese five-year bond yields. The estimation sample ranges from 04 January 2010 to 28 December 2012, except for Greece, for which the sample ends on 02 March 2012. Standard errors are in parentheses and are constructed from the numerical second derivatives of the log-likelihood function.

| | t-GAS volatility model | | | | |
|---|---|---|---|---|---|
| | $\omega_v$ | $a_v$ | $b_v$ | $\nu$ | LogLik |
| ES | -0.2360 | 0.2180 | 0.9377 | 2.5000 | 84766.1 |
| | (0.0115) | (0.0052) | (0.0030) | (0.0000) | |
| GR | -0.2565 | 0.3236 | 0.9207 | 2.5000 | 39844.0 |
| | (0.0113) | (0.0065) | (0.0034) | (0.0000) | |
| IE | -0.2644 | 0.3047 | 0.9283 | 2.5000 | 73240.1 |
| | (0.0099) | (0.0051) | (0.0026) | (0.0000) | |
| IT | -0.1667 | 0.1854 | 0.9558 | 2.5000 | 86264.8 |
| | (0.0094) | (0.0051) | (0.0024) | (0.0000) | |
| PT | -0.3146 | 0.3700 | 0.9071 | 2.5000 | 63207.3 |
| | (0.0098) | (0.0055) | (0.0028) | (0.0000) | |

| | Dynamic tail shape model (95%) | | | | |
|---|---|---|---|---|---|
| | $\omega$ | $a$ | $b$ | LogLik | $\exp\left(\frac{\omega}{1-b}\right)$ |
| ES | -0.0453 | 0.0013 | 0.9652 | -7421.7 | 0.27 |
| | (0.0142) | (0.0015) | (0.0109) | | |
| GR | 0.0000 | 0.0029 | 1.0000 | -9686.9 | 0.49 |
| | (0.0001) | (0.0005) | (0.0001) | | |
| IE | -0.0454 | 0.0000 | 0.9548 | -10937.2 | 0.37 |
| | (0.0178) | (0.0000) | (0.0177) | | |
| IT | -0.0008 | 0.0016 | 0.9994 | -8055.8 | 0.26 |
| | (0.0005) | (0.0004) | (0.0004) | | |
| PT | -0.0001 | 0.0017 | 0.9999 | -11978.6 | 0.37 |
| | (0.0001) | (0.0004) | (0.0001) | | |

| | Dynamic tail model (95%) with changes in SMP amounts | | | | | | |
|---|---|---|---|---|---|---|---|
| | $\omega$ | $a$ | $b$ | $c$ | $d$ | $e$ | LogLik |
| ES | -0.0005 | 0.0011 | 0.9996 | 0.0053 | -0.0253 | 0.1018 | -7400.2 |
| | (0.0004) | (0.0003) | (0.0003) | (0.0432) | (0.1484) | (0.1474) | |
| GR | 0.0000 | 0.0028 | 1.0000 | -0.0498 | 0.0114 | -0.0114 | -9686.1 |
| | (0.0000) | (0.0005) | (0.0000) | (0.0459) | (0.1732) | (0.1718) | |
| IE | -0.0002 | 0.0013 | 0.9998 | -0.0626 | 0.1959 | -0.1613 | -10881.2 |
| | (0.0002) | (0.0004) | (0.0002) | (0.0331) | (0.1223) | (0.1214) | |
| IT | -0.0008 | 0.0016 | 0.9994 | 0.0222 | -0.2098 | 0.2780 | -8052.3 |
| | (0.0005) | (0.0004) | (0.0004) | (0.0430) | (0.1438) | (0.1422) | |
| PT | -0.0001 | 0.0017 | 0.9999 | -0.0522 | -0.1510 | 0.1766 | -11975.9 |
| | (0.0001) | (0.0004) | (0.0001) | (0.0293) | (0.1180) | (0.1176) | |

Spain and Ireland. This outcome is robust to considering levels instead of changes, and to replacing the changes in volumes with dummies indicating the presence of the ECB in the respective markets; see Ghysels et al. (2016). As a result, the direct inclusion of SMP variables does not influence the fit of the dynamic tail index model to a large extent. This finding does not mean that purchases had no impact on the tail shape. Instead, carefully chosen control covariates are required.

## 4.3 SMP impact on tail risk

We explore the association of SMP purchases with tail risk by estimating the univariate time series regression

$$\hat{\xi}_t^D = \beta_0 + \beta_1 \hat{\xi}_{t-1}^D + \beta_2 \text{SMP}_t + \beta_3 \text{SMP}_{t-1} + \beta_4 \text{D}\{\text{OMT}_t\} + \epsilon_t, \tag{13}$$

where $\hat{\xi}_t^D = 1000 \times (\hat{\xi}_t^R - \hat{\xi}_t^L)$ is the scaled-up difference, in levels, between the estimate of the right (bad) tail shape parameter $\hat{\xi}_t^R$ and the tail shape $\hat{\xi}_t^L$ for the left (good) tail, for a particular bond market. The respective threshold value $\tau$ is taken as the empirical 5% percentile, implying two positive POT values per day on average. Regression 13 is specified at the daily frequency.

Considering the difference $\hat{\xi}_t^R - \hat{\xi}_t^L$ treats $\hat{\xi}_t^L$ as a control covariate which helps explain the time variation in $\hat{\xi}_t^R$, but is not, or much less, impacted by asset purchases.[4] On the right hand side, $\text{SMP}_t$ denotes the total amount spent on SMP purchases, in €billion of par value, in a certain bond market (all maturities) on intervention day $t$. The dummy variable $\text{D}\{\text{OMT}_t\}$ indicates the period after the ECB's announcement of the technical details of its OMT programme on 06 September 2012.

The top panel in Table 4 reports the parameter estimates for (13) obtained by least squares regression. The estimates suggest that ECB asset purchases within the SMP had an

[4]The ECB's first SMP announcement on 10 May 2010 made it clear that purchased bonds would be retired on its balance sheet until the bonds mature. The ECB never sold (nor lent out) any government bonds purchased within the SMP. As a result, the central bank purchases 'leaned against' sharply rising yields during the sovereign debt crisis.

impact on the tail risk of holding sovereign bonds in some countries, but not necessarily in others. The impact coefficient $\beta_3$ is significant for Greek and Spanish bonds, and insignificant for Portuguese, Irish, and Italian bonds. In addition, changes in tail risk are associated with lagged, not contemporaneous, purchases. This is not surprising, as $\hat{\xi}_t^R$ is a filtered (backward-looking) estimate. Future (smaller) exceedances are required to lower the dynamic tail shape parameter.

The time after the announcement of the OMT programme also appears to be associated with falling tail risk. The respective coefficient estimates are all of negative sign. However, they are statistically insignificant in all but one case (ES). No estimate for OMT impact is available for Greek bonds, as these discontinued trading during much of 2012.

To give the tail shape parameter more time to adjust to contemporaneous ECB actions, we consider two-day (34 hour) tail differences as a dependent variable. Thus, we compare the tail shape parameter estimates at the end of $t$ (6pm) with the estimate at the start of day $t-1$ (8am). We benchmark this difference by the corresponding difference in the left-hand (good) tail, again assuming that asset purchases affect mainly the right-hand tail by leaning against rising yields. As a result, we consider

$$\hat{\xi}_t^{DiD} = 1000 \times \left(\hat{\xi}_{t,6pm}^R - \hat{\xi}_{t-1,8am}^R\right) - \left(\hat{\xi}_{t,6pm}^L - \hat{\xi}_{t-1,8am}^L\right).$$

We then relate these (scaled-up) differences-in-differences to central bank unconventional policies according to

$$\hat{\xi}_t^{DiD} = \beta_0 + \beta_1 \hat{\xi}_{t-1}^{DiD} + \beta_2 \mathrm{SMP}_t + \beta_3 \mathrm{SMP}_{t-1} + \beta_4 \mathrm{SMP}_{t-2} + \beta_5 \mathrm{D}\{\mathrm{OMT}_t\} + \epsilon_t, \qquad (14)$$

where the right-hand side variables are defined as above.

The bottom panel of Table 4 presents the least squares parameter estimates for regression (14). The tail index differences remain somewhat autoregressive, with $\beta_1 \approx 0.5$. This value is approximately in line with the high-frequency estimates reported in Table 3, where, for example, $0.98^{4\times 10} \approx 0.45$. Coefficients for $\mathrm{SMP}_{t-1}$ are significantly negative for Spanish

Table 4: Regression estimates for tail risk differences

The top, middle, and bottom panel report least squares parameter estimates for univariate time series regressions (13), (14), and (17), respectively. Rows ES, GR, IE, IT, and PT refer to parameter estimates for Spanish, Greek, Irish, Italian, and Portuguese five-year benchmark bonds. Parameter t-values are in parentheses and are based on Newey-West HAC standard errors.

| | const. | $\hat{\xi}^{D}_{t-1}$ | $\text{SMP}_t$ | $\text{SMP}_{t-1}$ | $\text{D}\{\text{OMT}_t\}$ | $\text{R}^2$ |
|---|---|---|---|---|---|---|
| ES | 0.673 | 0.957 | 0.401 | -1.186 | -1.302 | 0.94 |
| | (3.08) | (86.3) | (0.88) | (-3.24) | (-2.41) | |
| GR | -0.035 | 0.984 | -0.003 | -0.028 | - | 0.99 |
| | (-2.24) | (86.1) | (-0.14) | (-2.47) | (-) | |
| IE | 0.438 | 0.982 | 0.376 | 0.300 | -0.803 | 0.97 |
| | (1.48) | (119.) | (0.14) | (0.13) | (-1.12) | |
| IT | 0.000 | 0.982 | 0.002 | 0.004 | -0.008 | 0.97 |
| | (0.15) | (119.) | (0.44) | (0.96) | (-1.12) | |
| PT | 0.549 | 0.983 | 1.605 | -1.567 | -0.158 | 0.96 |
| | (1.38) | (140.) | (1.19) | (-1.06) | (-0.19) | |

| | const. | $\hat{\xi}^{DiD}_{t-1}$ | $\text{SMP}_t$ | $\text{SMP}_{t-1}$ | $\text{SMP}_{t-2}$ | $\text{D}\{\text{OMT}_t\}$ | $\text{R}^2$ |
|---|---|---|---|---|---|---|---|
| ES | 0.537 | -0.049 | -0.345 | -0.625 | -0.013 | 0.032 | 0.29 |
| | (21.60) | (-0.31) | (-0.45) | (-1.94) | (-0.03) | (0.06) | |
| GR | 0.616 | -0.010 | -0.041 | -0.001 | 0.020 | - | 0.39 |
| | (11.60) | (-0.85) | (-2.54) | (-0.05) | (1.10) | - | |
| IE | 0.528 | 0.082 | -1.819 | 3.405 | -4.562 | -0.389 | 0.28 |
| | (23.40) | (0.34) | (-0.68) | (0.98) | (-2.66) | (-0.49) | |
| IT | 0.522 | 0.000 | -0.001 | 0.007 | -0.003 | -0.005 | 0.28 |
| | (18.20) | (-0.08) | (-0.15) | (1.42) | (-0.75) | (-0.69) | |
| PT | 0.532 | 0.041 | 0.593 | -3.530 | 1.943 | -0.494 | 0.28 |
| | (18.40) | (0.15) | (0.35) | (-3.37) | (1.16) | (-0.58) | |

| | const. | $\text{ES}^{DiD}_{t-1}$ | $\text{SMP}_t$ | $\text{SMP}_{t-1}$ | $\text{SMP}_{t-2}$ | $\text{D}\{\text{OMT}_t\}$ | $\text{R}^2$ |
|---|---|---|---|---|---|---|---|
| ES | 0.562 | -1.153 | -3.242 | -5.550 | 0.262 | 0.402 | 0.32 |
| | (19.60) | (-0.70) | (-0.46) | (-1.73) | (0.05) | (0.09) | |
| GR | 0.618 | 1.724 | -12.509 | -5.492 | 10.131 | - | 0.39 |
| | (9.65) | (1.32) | (-4.05) | (-0.93) | (1.98) | - | |
| IE | 0.521 | 1.503 | -28.750 | 60.792 | -72.732 | -7.303 | 0.27 |
| | (22.20) | (0.44) | (-0.71) | (1.18) | (-3.07) | (-0.63) | |
| IT | 0.473 | -0.205 | 0.153 | -1.001 | 1.076 | -0.926 | 0.23 |
| | (11.60) | (-0.37) | (0.16) | (-1.17) | (1.60) | (-1.26) | |
| PT | 0.538 | 1.514 | 7.375 | -56.986 | 37.129 | -8.796 | 0.29 |
| | (15.00) | (0.35) | (0.30) | (-3.69) | (1.50) | (-0.61) | |

and Portuguese tail risk differences at the 10% and 5% level, respectively. Greek tail risk differences respond negatively to contemporaneous purchases on the same day. For Irish bonds, we obtain a significant impact on tail risk at the one day lag.[5] For Italy, no entry

[5]These differences in time profiles of the impact probably reflect the statistical fact that our filtered estimates of $\xi_t$ require some time to react to future lower POT values, rather than structural economic differences, such as differences in the market microstructure of sovereign bond markets.

is statistically significant. This negative finding is approximately in line with the empirical results in Ghysels et al. (2016) and Eser and Schwaab (2016), where the smallest impact estimate (per €1 bn) on the conditional mean is obtained for these bonds.

The OMT level dummy again does not appear to be significantly related to time-variation in tail risk. However, the sign of the respective impact is negative in three out of four cases. We conclude that ECB asset purchases within the SMP had an impact on the tail risk of holding sovereign bonds, including the risk of making the respective markets, in most countries. The evidence regarding a pronounced tail risk impact from the ECB's OMT program is relatively weak.

## 4.4 SMP impact on market risk

This section quantifies the impact of SMP purchases on market risk measures such as Value-at-Risk (VaR) and Expected Shortfall (ExS) associated with holding certain SMP government bonds between 2010–2013. The measurement of market risk from holding certain financial instruments is a major application of EVT methods in practise; see McNeil et al. (2010).

A useful relationship between the GPD and excess loss measures is presented in McNeil and Frey (2000); see also Rocco (2014). In our setting, the VaR of $y_t$ at quantile $\gamma$ can be estimated as

$$\mathrm{VaR}_t^{\gamma}(Y) = \hat{\sigma}_t \tau + \frac{\hat{\sigma}_t}{\hat{\xi}_t} \left[ \left( \frac{N}{N_\tau} (1-\gamma)^{-\hat{\xi}_t} \right) - 1 \right], \tag{15}$$

where $\hat{\sigma}_t$ is obtained from (12), and $\tau$ is fixed for a given sample of size $N = t$ at time $t$. As the sample grows, time variation in $\tau$ is present but minimal, as it refers to devolatized data $x_t$ from a large sample at a high frequency. For any sample of size $N = t$, we observe $N_\tau$ non-zero observation for $x_t$. The corresponding ExS is the average VaR in the tail, see McNeil, Frey, and Embrechts (2010, Chapter 2), and can be obtained in closed form as

$$\mathrm{ExS}_t^{\gamma}(Y) = \frac{1}{1-\gamma} \int_{\gamma}^{1} \mathrm{VaR}_t^{\tau}(Y) \mathrm{d}\tau = \frac{\mathrm{VaR}_t^{\gamma}(Y)}{1-\hat{\xi}_t} + \frac{\hat{\sigma}_t (1 - \hat{\xi}_t \tau)}{1-\hat{\xi}_t}. \tag{16}$$

The ExS (16) is strictly higher than the VaR at the same confidence level, and "looks further into the tail" of rising yields.

Figure 4 plots our time series estimates of VaR and ExS at a 99% confidence level for five SMP benchmark bonds. We focus on three findings. First, government bonds differed substantially in terms of their tail risk at any given time during the euro area sovereign debt crisis. Italian and Spanish bonds have the lowest estimated ExS, with a risk of an increase of up to approximately 50 bps on average within 15 minutes at the 1% confidence level, particularly during 2011. Ireland and Portugal are intermediate cases, with a 15 minute 99% ExS of up to approximately 150 bps. Finally, Greek bonds had the highest estimated 15 minute ExS of up to approximately 300 bps, leading up to the eventual credit event in March 2012. For anecdotal evidence that market makers retreated from trading in the Italian debt securities in 2011 see Pelizzon, Subrahmanyam, Tomio, and Uno (2013).

Second, Figure 4 reveals a different timing of the maximum amount of financial stress in each market. Highest tail risks in terms of VaR and ExS are observed relatively late in Spain and Italy, with clear peaks in 2011Q4. In contrast, elevated market stress is visible for Greek, Irish and Portuguese bonds already much earlier, between 2010 – 2011. This is approximately in line with standard accounts of the debt crisis; see, for example, Cœuré (2013). Finally, outright purchases within the SMP visibly reduced the VaR and ExS of SMP bonds; see particularly Greek, Irish, and Portuguese bonds during 2010 and 2011, and Italian and Spanish bonds in 2011.

Finally, we test the impact of ECB non-standard policy measures on the market risk measures. To this purpose we follow the same empirical strategy as in Section 4.3. I.e., we again benchmark the right (bad) tail risk measure to its left-tail value, and consider two-day (34 hour) time differences, as $\mathrm{ExS}_t^{DiD} = 1000\times\big(\mathrm{ExS}_{t,6pm}^{R} - \mathrm{ExS}_{t-1,8am}^{R}\big) - \big(\mathrm{ExS}_{t,6pm}^{L} - \mathrm{ExS}_{t-1,8am}^{L}\big)$. We relate these differences in market risk to unconventional policies as

$$\mathrm{ExS}_t^{DiD} = \beta_0 + \beta_1 \mathrm{ExS}_{t-1}^{DiD} + \beta_2 \mathrm{SMP}_t + \beta_3 \mathrm{SMP}_{t-1} + \beta_4 \mathrm{SMP}_{t-2} + \beta_5 \mathrm{D}\{\mathrm{OMT}_t\} + \epsilon_t, \quad (17)$$

where the right-hand side variables are defined as above.

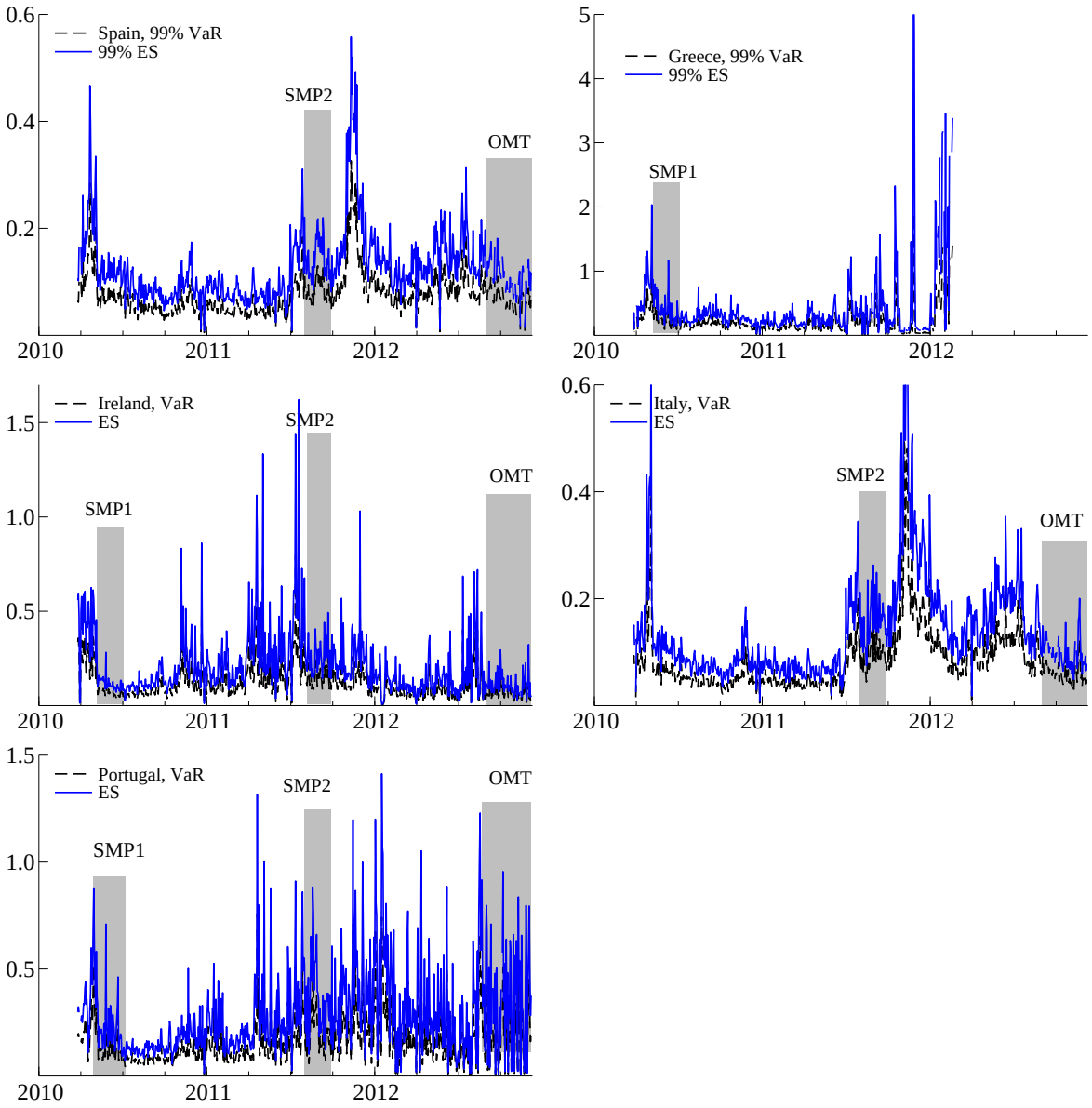


Figure 4: VaR and ExS estimates for five SMP bonds

Value-at-Risk (VaR) and Expected Shortfall (ES) estimates for five-year benchmark government bonds for Spain (ES), Greece (GR), Ireland (IE), Italy (IT), and Portugal (PT). We compute the VaR and ES at a 99% confidence level, based on tail shape estimates $\hat{\xi}_t$ obtained at the 5% quantile. Shaded areas correspond to policy interventions. Data between 01 January and 30 March 2010 are used to initiate the threshold $\tau$, and are not reported. We report the daily median value of the 15 minute estimates.

The bottom panel of Table 4 reports the regression outcomes for (17).[6] The parameter estimates are similar to our earlier findings from regression (14). The ExS is reduced for almost all countries, except Italy, following SMP interventions. Differences in timing exist, and may be related to the fact that ExS is based on filtered parameter estimates obtained from sparse tail observations. The regression estimates for VaR differences are similar and therefore omitted. We conclude that the SMP programme contributed towards mitigating high tail risk in government bond markets during the sovereign debt crisis between 2010-2012.

# 5 Conclusion

This paper introduced time variation into the tail index parameter of the Generalized Pareto Distribution, yielding a novel observation-driven model. Monte Carlo experiments suggest that our approach reliably captures tail shape variation in different environments. In an empirical application, we demonstrated that asset purchases within the ECB's SMP are associated with declining tail risk associated with holding certain sovereign bonds during the euro area sovereign debt crisis between 2010–2012.

# References


Adrian, T. and H. S. Shin (2010). Liquidity and leverage. *Journal of Financial Intermediation 19*(3), 418–437.

Allen, L., T. G. Bali, and Y. Tang (2012). Does systemic risk in the financial sector predict future economic downturns? *Review of Financial Studies 25*(10), 3000–3036.

Blasques, F., S. J. Koopman, and A. Lucas (2015). Information theoretic optimality of observation driven time series models for continuous responses. *Biometrika 102*(2), 325–343.

Brownlees, C. T. and R. Engle (2015). SRisk: A conditional capital shortfall index for systemic risk measurement. *Unpublished working paper*.


[6] We use the risk measures from the filtered yield returns for this purpose; i.e., $\hat{\sigma}_t = 1$ in (15) and (16). Otherwise, any SMP impact on the conditional variance would influence the left tail value as well. The ExS is at the 1% level.

Cœuré, B. (2013). Outright Monetary Transactions, one year on. Speech at the conference "The ECB and its OMT programme," Berlin, 2 September 2013.

Cox, D. R. (1981). Statistical analysis of time series: some recent developments. *Scandinavian Journal of Statistics 8*, 93–115.

Creal, D., S. J. Koopman, and A. Lucas (2013). Generalized autoregressive score models with applications. *Journal of Applied Econometrics 28*(5), 777–795.

Creal, D., B. Schwaab, S. J. Koopman, and A. Lucas (2014). An observation driven mixed measurement dynamic factor model with application to credit risk. *The Review of Economics and Statistics 96(5)*, 898915.

Davidson, A. C. and R. L. Smith (1990). Models for exceedances over high thresholds. *Journal of the Royal Statistical Association, Series B 52*(3), 393442.

ECB (2013). European Central Bank Annual Report 2012.

Embrechts, P., C. Klüppelberg, and T. Mikosch (1997). *Modelling extremal events for insurance and finance*. Springer Verlag, Berlin.

Eser, F., M. Carmona Amaro, S. Iacobelli, and M. Rubens (2012). The use of the Eurosystem's monetary policy instruments and operational framework since 2009. ECB Occasional Paper 135, European Central Bank.

Eser, F. and B. Schwaab (2016). Evaluating the impact of unconventional monetary policy measures: Empirical evidence from the ecb's securities markets programme. *Journal of Financial Economics 119*(1), 147167.

Galbraith, J. W. and S. Zernov (2004). Circuit breakers and the tail index of equity returns. *Journal of Financial Econometrics 2*(1), 109–129.

Ghysels, E., J. Idier, S. Manganelli, and O. Vergote (2016). A high frequency assessment of the ecb securities markets programme. *Journal of European Economic Association, forthcoming*.

González-Páramo, J.-M. (2011). The ECB's monetary policy during the crisis. Closing speech at the Tenth Economic Policy Conference, Málaga, 21 October 2011.

Hartmann, P., S. Straetmans, and C. de Vries (2004). Asset market linkages in crisis periods. *Review of Economics and Statistics 86(1)*, 313–326.

Hartmann, P., S. Straetmans, and C. de Vries (2007). Banking system stability: A cross-atlantic perspective. In M. Carey and R. M. Stulz (Eds.), *The Risks of Financial Institutions*, pp. 1–61. NBER and University of Chicago Press.

Harvey, A. C. (2013). *Dynamic models for volatility and heavy tails: with applications to financial and economic time series*. Number 52. Cambridge University Press.

Kelly, B. (2014). The dynamic power law model. *Extremes 17*(4), 557–583.

Kelly, B. and H. Jiang (2014). Tail risk and asset prices. *Review of Financial Studies*, hhu039.

Lucas, A., B. Schwaab, and X. Zhang (2014). Conditional euro area sovereign default risk. *Journal of Business and Economics Statistics 32*(2), 271–284.

Lucas, A., B. Schwaab, and X. Zhang (2016). Modeling financial sector joint tail risk in the euro area. *Journal of Applied Econometrics, forthcoming*.

Massacci, D. (2014). Tail risk dynamics in stock returns: Observation driven approach and links to the business cycle. Technical report.

McNeil, A. and R. Frey (2000). Estimation of tail-related risk measures for heteroscedastic financial time series: An Extreme Value Approach. *Journal of Empirical Finance 7*(3-4), 271–300.

McNeil, A. J., R. Frey, and P. Embrechts (2010). *Quantitative risk management: concepts, techniques, and tools*. Princeton university press.

Poon, S., M. Rockinger, and J. Tawn (2004). Extreme value dependence in financial markets. *Review of Financial Studies 17(2)*, 581–610.

Quintos, C., Z. Fan, and P. C. Phillips (2001). Structural change tests in tail behaviour and the asian crisis. *The Review of Economic Studies 68*(3), 633–663.

Rocco, M. (2014). Extreme value theory in finance: A survey. *Journal of Economic Surveys 28*(1), 82–108.

Vayanos, D. and J.-L. Vila (2009). A preferred habitat model of the term structure of interest rates. NBER Working Paper 15487.

Wagner, N. (2005). Autoregressive conditional tail behavior and results on government bond yield spreads. *International Review of Financial Analysis 14*(2), 247–261.

Werner, T. and C. Upper (2004). Time variation in the tail behavior of bund future returns. *Journal of Futures Markets 24*(4), 387–398.

# Appendix A1: Score and scaling function for GPD distribution

This section derives (4) – (5). Recall that the log-density is given by (2) as $l(x_t;\delta,\xi_t) = -\ln(\delta) - \left(1+\frac{1}{\xi_t}\right)\ln\left(1+\xi_t\frac{x_t}{\delta}\right)$, where $\delta > 0$, $\xi_t > 0$, $x_t > 0$, and $\xi_t = \exp(f_t)$. The score dynamics (4) are straightforward, and are obtained as

$$\begin{aligned}
\nabla_t &= \frac{\partial l(x_t;\delta,\xi_t)}{\partial f_t} = \frac{\partial l(x_t;\delta,\xi_t)}{\partial \xi_t}\cdot\frac{\mathrm{d}\xi_t}{\mathrm{d}f_t},\\
\frac{\partial l(x_t;\delta,\xi_t)}{\partial \xi_t} &= \frac{1}{\xi_t^2}\ln\left(1+\xi_t\frac{x_t}{\delta}\right) - \left(1+\frac{1}{\xi_t}\right)\frac{x_t}{\delta+\xi_t x_t},\\
\frac{\mathrm{d}\xi_t}{\mathrm{d}f_t} &= \exp(f_t).
\end{aligned}$$

The score is zero in expectation, assuming that the model is well-specified; see Creal et al. (2013). This implies

$$\int_0^\infty \frac{1}{\xi_t^2}\ln\left(1+\xi_t\frac{x_t}{\delta}\right)p(x_t;\delta,\xi_t)\mathrm{d}x_t = \int_0^\infty \left(1+\frac{1}{\xi_t}\right)\frac{x_t}{\delta+\xi_t x_t}p(x_t;\delta,\xi_t)\mathrm{d}x_t. \tag{A1}$$

The scaling function is chosen as the inverse conditional Fisher information of the GPD,

$$\mathcal{S}_t = \mathrm{E}[\nabla_t^2|\mathcal{F}_{t-1};f_t,\psi]^{-1} = \mathrm{E}\left[\left(\frac{\partial l(x_t;\delta,\xi_t)}{\partial\xi_t}\right)^2\left(\frac{\mathrm{d}\xi_t}{\mathrm{d}f_t}\right)^2\right]^{-1} = \mathrm{E}\left[-\frac{\partial^2 l(x_t;\delta,\xi_t)}{\partial\xi_t^2}\right]^{-1}\exp(-2f_t).$$

The expected negative second derivative is given by

$$\begin{aligned}
\mathrm{E}\left[-\frac{\partial^2 l(x_t;\delta,\xi_t)}{\partial\xi_t^2}\right] &= -\int_0^\infty\left[\left(1+\frac{1}{\xi_t}\right)\frac{x_t^2}{(\delta+\xi_t x_t)^2} + \frac{2}{\xi_t^2}\frac{x_t}{\delta+\xi_t x_t} - \frac{2}{\xi_t^3}\ln\left(1+\xi_t\frac{x_t}{\delta}\right)\right]p(x_t;\delta,\xi_t)\mathrm{d}x_t\\
&= -\int_0^\infty\left[\left(1+\frac{1}{\xi_t}\right)\frac{x_t^2}{(\delta+\xi_t x_t)^2} + \frac{2}{\xi_t^2}\frac{x_t}{\delta+\xi_t x_t} - \frac{2}{\xi_t}\left(1+\frac{1}{\xi_t}\right)\frac{x_t}{\delta+\xi_t x_t}\right]p(x_t;\delta,\xi_t)\mathrm{d}x_t\\
&= -\int_0^\infty\left[\left(1+\frac{1}{\xi_t}\right)\frac{x_t^2/\delta^2}{(1+\xi_t x_t/\delta)^2} - \frac{2}{\xi_t}\frac{x_t/\delta}{1+\xi_t x_t/\delta}\right]\frac{1}{\delta}\left(1+\xi_t\frac{x_t}{\delta}\right)^{-\frac{1}{\xi_t}-1}\mathrm{d}x_t\\
&= -\int_0^\infty\left[\left(\frac{1+\xi_t}{\xi_t^3}\right)\frac{\xi_t^2 x_t^2/\delta^2}{(1+\xi_t x_t/\delta)^2} - \frac{2}{\xi_t^2}\frac{\xi_t x_t/\delta}{1+\xi_t x_t/\delta}\right]\frac{1}{\delta}\left(1+\xi_t\frac{x_t}{\delta}\right)^{-\frac{1}{\xi_t}-1}\mathrm{d}x_t\\
&= -\frac{1+\xi_t}{\xi_t^4}\int_1^\infty(\tilde{x}_t-1)^2\tilde{x}_t^{-1/\xi_t-3}\mathrm{d}\tilde{x}_t + \frac{2}{\xi_t^3}\int_1^\infty(\tilde{x}_t-1)\tilde{x}_t^{-1/\xi_t-2}\mathrm{d}\tilde{x}_t,
\end{aligned} \tag{A2}$$

where we used (A1) in the second line, and where the last equality comes from a change of variable substituting $\tilde{x}_t = 1+\xi_t x_t/\delta$.

The two integrals in (A2) can be treated as functions of moments $\mathrm{E}(\tilde{x}_t)$. To see this, note that the new random variable $\tilde{x}_t$ is Pareto (Type 1) distributed, with pdf

$$\tilde{p}(\tilde{x}_t; a_t, b) = \frac{a_t b^{a_t}}{\tilde{x}_t^{a_t+1}}, \qquad \tilde{x}_t > 1, \tag{A3}$$

with $n$th un-centered moment available as

$$\mathrm{E}(\tilde{x}_t^n) = \frac{a_t b^n}{a_t - n}. \tag{A4}$$

The first integral in (A2) corresponds to $\tilde{p}(\tilde{x}_t; 1/\xi_t + 2, 1)$. The second integral corresponds to $\tilde{p}(\tilde{x}_t; 1/\xi_t + 1, 1)$, such that

$$\begin{aligned} -\frac{1+\xi_t}{\xi_t^4} \int_1^\infty (\tilde{x}_t - 1)^2 \tilde{x}_t^{-1/\xi_t - 3} \mathrm{d}\tilde{x}_t &= \frac{-2}{\xi_t(1+2\xi_t)} \\ \frac{2}{\xi_t^3} \int_1^\infty (\tilde{x}_t - 1) \tilde{x}_t^{-1/\xi_t - 2} \mathrm{d}\tilde{x}_t &= \frac{2}{\xi_t(1+\xi_t)}. \end{aligned}$$

Reorganizing terms, we obtain the scaling function (5) in closed form as

$$\mathcal{S}_t = \frac{(1+2\xi_t)(1+\xi_t)}{2} \exp\left(-2f_t\right) = \frac{(1+2\xi_t)(1+\xi_t)}{2\xi_t^2}.$$